

## SIMULATION OF GAS TEMPERATURE VARIATION AND DIFFUSION EFFECTS IN AN AIR CORONA DISCHARGE FOR NO<sub>x</sub> POLLUTION CONTROL

Nanang Arif Guntoro<sup>1\*</sup>

<sup>1</sup>*Department of Electrical Engineering, Faculty of Engineering, Jakarta State University, Indonesia*

### ABSTRACT

The specificity of this research comes from the consideration of both the reactive neutral dynamics gas and the charged particle dynamics in order to study the channel reactions for NO<sub>x</sub> removal. A mass transfer simulation, including radial diffusion, gas temperature variation and chemical kinetics, is developed to follow the spatio-temporal evolution of the main neutral chemical species in a pulsed corona discharge used for NO<sub>x</sub> pollution control from oil or coal burning flue gases. The calculation has been performed in a simplified air-flue gas at atmospheric pressure and ambient temperature including 400ppm of NO. The diffusion coefficients of each neutral species are calculated by using the kinetics theory of gases. The temperature variations take into account the vibrational energy relaxation into random thermal energy. The numerical method used to solve the previous equations is presented while its efficiency is proved with two restricting tests which compare analytical and numerical solutions. The simulation takes into account 16 neutral chemical species reacting following 110 chemical reactions. The obtained results show that the diffusion and the temperature variations reduce significantly the oxide removal in the ionised channel. This tendency is reinforced by the enhancing of the gas temperature which increases the diffusion phenomena and reduces the efficiency of some important chemical reactions which participated in the oxide removal.

*Keywords:* Air corona discharge; Diffusion effects; Gas temperature variation; Mass transfer simulation; NO<sub>x</sub> pollution control

### 1. INTRODUCTION

The pulsed corona discharge is one of the nonthermal plasma technique which can be used to remove toxic oxides (such as NO<sub>x</sub>) from the polluted industrial flue gases [Penetrante and Schultheis, 2012]. In this technique, the toxins react with radicals species (such as O, N, OH) which are created in every filamentary plasma by electron- molecule and ion- molecule impacts. Reactions with radicals produce acids (such as HNO<sub>3</sub> which can be transformed into salt by adding a base) and other non-toxic atoms and molecules (like O, N, N<sub>2</sub>, CO<sub>2</sub>). During the pollution control process, the time needed to remove oxides by reactions with radicals is larger than diffusion time of main chemical species. Therefore, the radial expansion of the gas mixture in the discharge channel affects the chemical kinetics significantly [Gentile and Kushner, 2006]. Furthermore, a fraction of the dissipated power in the plasma channel relaxes into a thermal form. The resulting gas temperature rises greatly modifies the chemical kinetic and also the diffusion phenomena [Eichwald et al., 2010].

---

\* Corresponding author's email: [nanangarifguntoro@yahoo.co.id](mailto:nanangarifguntoro@yahoo.co.id)

In the present work, we study the effects of both the radial diffusion and gas temperature variation on the NO remediation in a pulsed air corona discharge at ambient temperature and atmospheric pressure.

The article is organized as follow: Section 2 is devoted to a description of our mathematical model of a reactive gas mixture including radial diffusion and gas temperature variation. In section 3, we describe the numerical method employed, and our simulation conditions. Then in section 4, some obtained results are shown and discussed before giving our concluding remarks.

## 2. DESCRIPTION OF THE MODEL

The 1D model is devoted the radial expansion (i.e. in a direction transversal to the discharge channel) of the reactive gas due to diffusion and temperature phenomena. The model assumes that the gas pressure remains constant. This assumption is valid in the major part of the interelectrode volume as the pressure waves, and the resulting convection phenomena occur mainly close to the anode.

The evolution of each chemical component in the mixture is described by the following mass conservation formulae:

$$\frac{\partial n_i}{\partial t} + \frac{1}{r} \frac{\partial}{\partial r} (n_i V_i) = S_i \quad , \quad i \in (n_p-1) \quad (1)$$

In this equation,  $n_i$  is the density of species  $i$  and  $n_p$  the number of chemical species in the gas mixture.  $r$  is the direction perpendicular to the streamer propagation axis. The total density  $n$  is given by the equation of state of an ideal gas:

$$P = nkT \quad (2)$$

$P$  is the pressure (pascal),  $k$  the Boltzmann constant and  $T$  the absolute temperature ( $^{\circ}\text{K}$ ). Term  $n_i V_i$  in equation (1) is the diffusive flux of chemical species  $i$  in the gas.  $V_i$  is the diffusion velocity, which can be calculated using the following diffusion equation:

$$n_i V_i = D_i \frac{\partial n_i}{\partial r} \quad (3)$$

$D_i$  is the diffusion coefficient of chemical species  $i$  in the mixture. In our model,  $D_i$  verifies the Blanc's Law:

$$D_i = \left[ \sum_{j \neq i} \left( \frac{n_j/n}{D_{ij}} \right) \right]^{-1} \quad (4)$$

$D_{ij}$  is the diffusion coefficient of species  $i$  and  $j$  in the corresponding binary mixture at temperature  $T$ .  $D_{ij}$  is estimated from the classical kinetic theory of gases [Hirschfelder et al., 1954] assuming that the potential field between the two colliding molecules is a Lennard-Jones 6-12 potential. Therefore,  $D_{ij}$  is given by the relation:

$$D_{ij} = 0,0026280 \frac{\sqrt{T^3 (M_i + M_j) / 2M_i M_j}}{P \sigma_{ij}^2 \Omega_{ij} (KT / \epsilon_{ij})} \quad (5)$$

$\Omega_{ij}$  is the (dimensionless) reduced collision integral, depending on the reduced temperature  $kT/\varepsilon_{ij}$ .  $M_i$  and  $M_j$  are the molecular masses ( $\text{g mol}^{-1}$ ) and the pressure  $P$  is expressed atmosphere.  $\sigma_{ij}$  is the collision diameter and  $\varepsilon_{ij}$  the maximum energy of attraction. The collision diameter  $\sigma_{ij}$  is evaluated as the arithmetic average of the appropriate  $\sigma$ -values for each gas i.e.  $\sigma_{ij}=(\sigma_i + \sigma_j)/2$ , and  $\varepsilon_{ij}$  is approximated as a geometric mean of the individual energies i.e.  $\varepsilon_{ij}=\sqrt{\varepsilon_i\varepsilon_j}$ . The source term  $S_i(T)$  in equation (1) corresponds to the gain and loss of species due to the chemical reactions [Eichwald, et al., 1999].

The modeling of the gas temperature variation includes the relaxation of electronic and vibrational energy extinction into random thermal energy. The fractions of energy transferred from charged to neutral particles via elastic and inelastic processes are given from a Boltzmann equation solution [Yousfi and Benabdessadok, 1996]. The gas temperature variation is obtained from:

$$\frac{\partial(\rho C_p T)}{\partial t} = (f_{ex} + f_t) J.E + \text{div}(\lambda(T) \text{grad}(T)) + \frac{\varepsilon_v}{\tau_v} \quad (6)$$

$$\frac{\partial \varepsilon_v}{\partial t} = f_v J.E - \frac{\varepsilon_v}{\tau_v} \quad (7)$$

$\rho$  is the mass density of the gas,  $C_p$  the heat capacity,  $J$  the current capacity,  $E$  the electric field, and  $\lambda(T)$  the thermal conductivity.

Equation (7) describes the evolution of the vibrational energy density  $\varepsilon_v$ ,  $f_t$  is the fraction of the dissipated power  $J.E$  used for the direct heating via elastic and rotational collisions. The fraction  $f_{ex}$  corresponds to the energy lost during to the electronic excitation and  $\tau_v$  the vibrational relaxation time which is chosen equal to  $50\mu\text{s}$ .

### 3. NUMERICAL METHOD AND SIMULATION CONDITIONS

Due to the rotational symmetry around the discharge propagation, the previous transport equations are integrated in a one-dimensional cylindrical geometry following radial  $r$  direction. The diffusive flux is corrected by the MUSCL superbee scheme [Leer, 1979] in order to limit the numerical diffusion. The time step evolution is calculated so that the maximum variation of any chemical species (due to either diffusive or kinetics phenomena) is less than 2%. The time step could be recalculated if it does not verify the classical CFL numerical criterion. The previous remark are summarised in Figure 1.

The considered flue gas is the synthetic dry air (80% of  $\text{N}_2$  and 20% of  $\text{O}_2$ ) involving 400ppm of NO at atmospheric pressure and ambient temperature. Our model takes into account 16 neutral chemical species {atoms N and O, molecules  $\text{N}_2$ ,  $\text{O}_2$ , NO,  $\text{O}_3$ ,  $\text{NO}_2$ ,  $\text{NO}_3$ ,  $\text{N}_2\text{O}$ ,  $\text{N}_2\text{O}_5$ ,  $\text{N}_2(\text{A}^3\text{S } u^+)$ ,  $\text{N}_2(\text{a}'^1\text{S } u^-)$ ,  $\text{O}_2(\text{a}^1\text{D } g)$ ,  $\text{N}(^2\text{D})$ ,  $\text{N}(^2\text{P})$ , and  $\text{O}(^1\text{D})$ } reacting following 110 selected chemical reactions. The Lennard-Jones parameters values used to calculate the diffusion coefficient of metastable species is chosen equal to the corresponding neutral ground species.

The simulation begins at 10ns and stops at 1ms. A 1,5D streamer model [Kanzari et al., 1998] coupled with a chemical kinetics model involving charged and exit particles give the initial density of each neutral species at 10ns. The radial density of charged particles has a Gaussian shape with a half width of  $100\mu\text{m}$ . The discharge characteristics are those of an experimental set-up [Dors and Mizeraczyk, 1998] (wire-cylinder geometry, interelectrode distance=1mm, pulse duration=10ns,  $V_{\text{max}}=10\text{kV}$ ) used for NO removal from flue gas. The discharge simulation is sustained after the end of the voltage pulsed in

order to take into account the power dissipated by the plasma during the extinction. Table 1 summarises the Lennard-Jones parameters values used to calculate the diffusion coefficient.

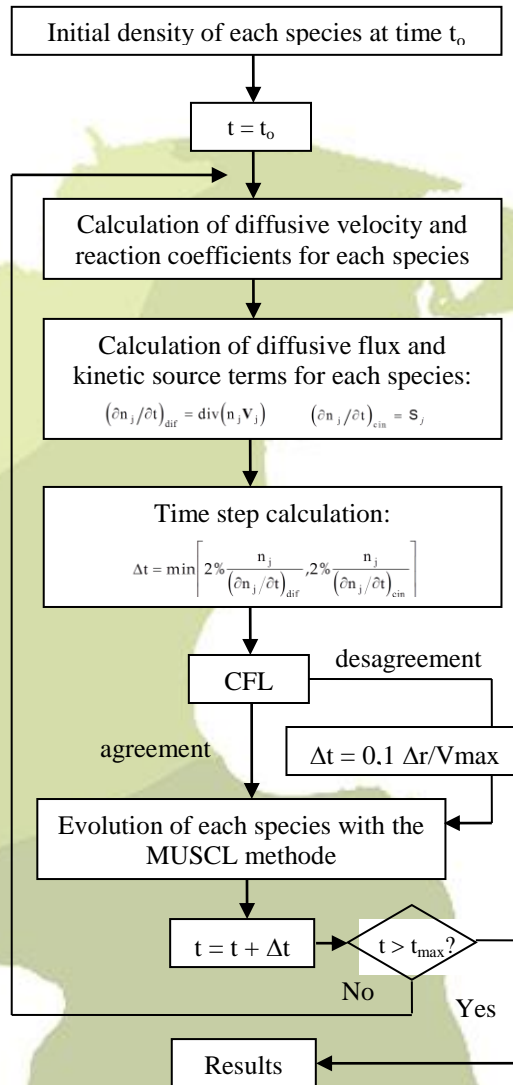


Figure 1: Flow chart for the simulation of the spatio-temporal evolution of a reactive gas mixture

Table 1: Values of the Lennard-jones potential parameters used to calculate the binary diffusion coefficients

	$\sigma$ (Å)	$\epsilon/k$ (°K)	References
N <sub>2</sub>	3.681	91.5	Hirschfelder et al., 1954
O <sub>2</sub>	3.433	113.0	Hirschfelder et al., 1954
NO	3.470	119.0	Hirschfelder et al., 1954
N	3.298	71.4	Svehla and Brokaw, 1996

	$\sigma$ (Å)	$\varepsilon/k$ (°K)	References
O	3.050	106.7	Svehla and Brokaw, 1996
O <sub>3</sub>	3.875	208.4	Massman, 1998
NO <sub>2</sub>	3.765	210.0	Svehla and Brokaw, 1996
NO <sub>3</sub>	3.770	395.0	Patrick and Golden, 1983

#### 4. RESULTS AND DISCUSSION

Figure 2 shows the radial gas temperature profile evolution. During the discharge phase in our simulation condition, the main part of the dissipated power (more than 95%) is transferred into vibrational excitation energy.

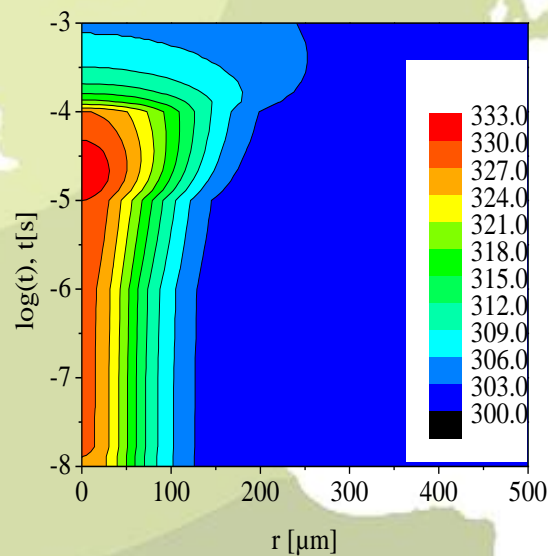


Figure 2: Radial gas temperature profile evolution (units in °K)

As this energy relaxes into a thermal form with a delay time of about  $50\mu\text{s}$ , the gas temperature reaches its maximum value ( $333^\circ\text{K}$ ) after about  $50\mu\text{s}$  on the discharge axis. In fact, the vibrational energy storage is maximum on the axis since the dissipated power profile follows the radial Gaussian shape of the electronic and ionic density into the channel. After  $50\mu\text{s}$ , the gas temperature on the axis decreases because of the thermal diffusion which also enlarges the radial gas temperature profile. We can notice that Figure 2 gives a direct information about the gas density profile (i.e. the density of the two main molecules  $\text{N}_2$  and  $\text{O}_2$ ). In fact, as the gas pressure remains constant, the gas density profile is the “negative” picture of the temperature profile since  $n=P/kT$ .

Figure 3 and 4 show respectively the radial density evolution of NO and  $\text{NO}_2$ : (a) without diffusion, and (b) with temperature variation and diffusion effects. The initial concentration of NO oxide is homogeneous and equal to 400ppm (see Figures 3 at 10ns) while the  $\text{NO}_2$  density is assumed negligible (see Figures 4). In the two considered cases (a and b) two main oxidation reactions ( $\text{O}+\text{NO}+\text{M}\rightarrow\text{NO}_2+\text{M}$  where M is either  $\text{N}_2$  or  $\text{O}_2$  and  $\text{O}_3+\text{NO}\rightarrow\text{NO}_2+\text{O}_2$ ) govern the NO and  $\text{NO}_2$  evolution. In case (a), the NO oxidation creates the  $\text{NO}_2$  molecules which reaches 32.4ppm after 1ms. Concurrently, the NO density decreases down to 400ppm at 1ms. In case (b), the NO removal around the axis is balanced by the diffusion of NO molecules from the discharge border towards the axis. This phenomenon prevails after  $10\mu\text{s}$  because the NO concentration gradients are high

enough to enhance the diffusion phenomena. Therefore the NO density reaches its minimum value (1.125ppm) on the axis at around  $10\mu\text{s}$ . In the same time, the radial diffusion of  $\text{NO}_2$  molecules limits their accumulation around the axis (the maximum value is of about 20.7ppm). Furthermore, after  $100\mu\text{s}$  the O radical is completely destroyed and can not therefore oxide (by reaction  $\text{O}+\text{NO}+\text{M}\rightarrow\text{NO}_2+\text{M}$ ) the additional NO molecules which diffuse from the gas towards the axis.

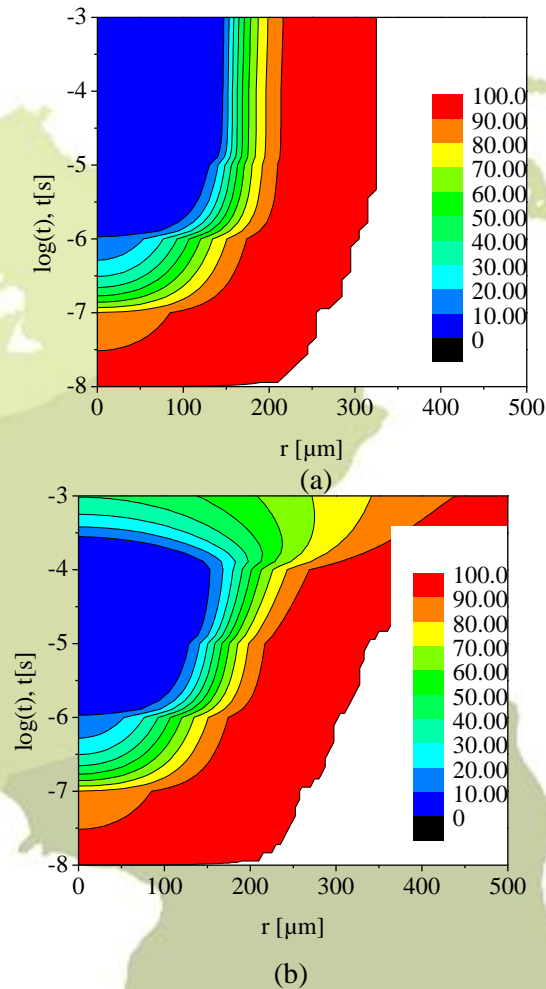


Figure 3: NO radial profil evolution (a) without diffusion ( $n_{\text{max}}=400$  ppm ;  $n_{\text{min}}=0.595$  ppm); (b) with temperature variation and diffusion effects ( $n_{\text{max}}=400$  ppm ;  $n_{\text{min}}=1.125$  ppm)

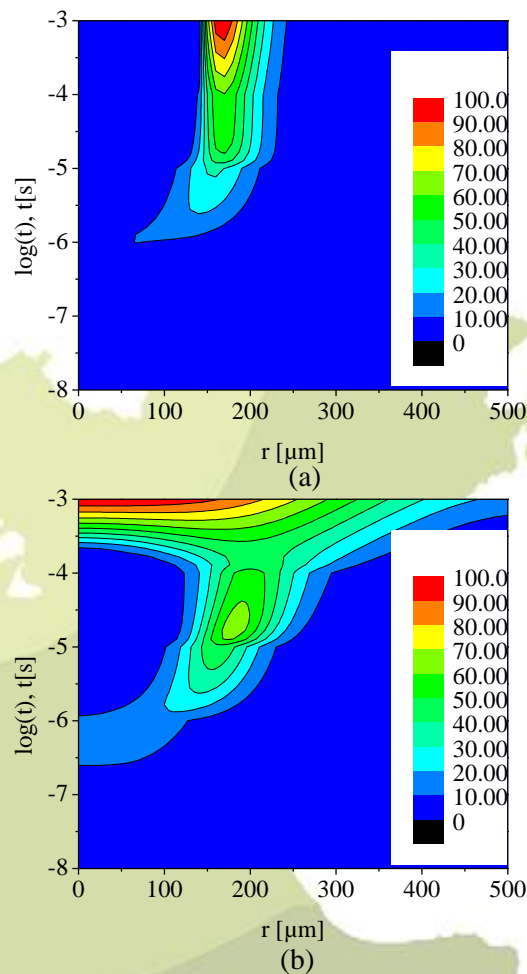


Figure 4: NO<sub>2</sub> radial profil evolution (a) without diffusion ( $n_{\max}=32.4$  ppm ;  $n_{\min}<0.001$  ppm); (b) with temperature variation and diffusion effects ( $n_{\max}=20.7$  ppm ;  $n_{\min}<0.001$  ppm)

The same phenomenon explain the evolution of NO and NO<sub>2</sub> oxides in case (b). However, there are amplified with the gas temperature rise. Therefore, the NO removal and the NO<sub>2</sub> creation are lower when the temperature variations are taken into account (see Figure 4). The minimum value of NO density is 1.125ppm around 10 $\mu$ s while the maximum value of NO<sub>2</sub> reaches 20.7ppm on the axis at the same time. In fact, the temperature rise enhances the diffusion phenomena which balance the NO reduction on the axis and the limit accumulation of NO<sub>2</sub>. As the diffusion velocity is larger with the temperature increase, the radial profile of NO and NO<sub>2</sub> oxides is more extended than in the case of a constant gas temperature (see Figures 3b and 4b). Furthermore, the decrease of the gas density (due to a higher temperature) reduces the NO oxidation by the three body reaction  $O+NO+M\rightarrow NO_2+M$  whose the efficiency is also reduced when the gas temperature increases. Finally, the diffusion rise limits the accumulation of the O<sub>3</sub> radical around the axis thus limiting the NO<sub>2</sub> creation by the reaction  $O_3+NO\rightarrow NO_2+O_2$ .

## 5. CONCLUSION

The present results show that gas temperature rise, mainly due to the vibrational energy relaxation in our simulation conditions, increases the mass diffusion phenomena and reduces the efficiency of the NO oxidation reaction, thus limiting the NO removal in the discharge channel. The present model gives information along the radial direction perpendicular to the streamer propagation. In order to include the axial heregonity (of dissipated power, pressure waves, and radical species distribution) we plane to develop a 3D model able to take into account the oxides localisation in the whole discharge volum.

## 6. REFERENCES

- Dors, M., and Mizeraczyk J., (1998), Czechoslovak Journal of Physics, 48 (10), 1193
- Eichwald, O., Yousfi, M., Hennad, A., and Benabdessadok, M. D., (1999), Journal Applied Physics, 82 (10), 4781
- Eichwald, O., Guntoro, N.A., Yousfi, M., and Benhenni, M., (2010), XIII Int. Conf. Gas Discharges and Their Applications, Vol.2, p.732-735
- Gentile, A.C., and Kushner, M.J., (2006), Journal Applied Physics 79 (8), 3877
- Hirschfelder, J.O., Curtiss, F.E., and Bird, R.B., (1954), Molecular Theory of Gases and Liquids, John Wiley-New York, Chapman et Hall, London
- Kanzari, Z., Yousfi, M., and Hamani, A., (1998), Journal Applied Physics, 84 (8), 4161
- Leer, B.V., (1979), Journal Computational Physics, 32, 101
- Massman, W.J., (1998), Atmospheric Environment, 32, pp.1111-1127
- Patrick, R., and Golden, D.M., (1983), International Journal Chemichal Kinetics, 15, pp.1189-1227
- Penetrante, B.M., and Schultheis, S.E., (2012), Non Thermal Plasma Techniques for Pollution Control, Springer, New York
- Svehla, A.R., and Brokaw, R.S., (1996), NASA Lewis Research Center, Cleveland, Ohio, NASA Technical Note, NASA TN D-3327
- Yousfi, M., and Benabdessadok M.D., (1996), Journal Applied Physics, 80, 6619